Hindawi
Journal of Advanced Transportation
Volume 2019, Article ID 4023970, 17 pages
https://doi.org/10.1155/2019/4023970

Research Article

Drivers' Braking Behaviors in Different Motion Patterns of Vehicle-Bicycle Conflicts

Lian Hou,[1] **Jingliang Duan**,[1] **Wenjun Wang**,[1] **Renjie Li**,[1] **Guofa Li**,[2] **and Bo Cheng**[1]

[1] *State Key Laboratory of Automotive Safety and Energy, Department of Automotive Engineering, Tsinghua University, Beijing 100084, China*
[2] *Institute of Human Factors and Ergonomics, College of Mechatronics and Control Engineering, Shenzhen University, Shenzhen 518060, China*

Correspondence should be addressed to Wenjun Wang; wangxiaowenjun@tsinghua.edu.cn

Received 28 August 2018; Accepted 5 February 2019; Published 3 March 2019

Academic Editor: Alain Lambert

Bicycling is one of the popular modes of transportation, but bicyclists are easily involved in injuries or fatalities in vehicle-bicycle (V-B) accidents. The AEB (Autonomous Emergency Braking) systems have been developed to avoid collisions, but their adaptiveness needs to be further improved under different motion patterns of V-B conflicts. This paper analyzes drivers' braking behaviors in different motion patterns of V-B conflicts to improve the performance of Bicyclist-AEB systems. For safety and data reliability, a driving simulator was used to reconstruct two typical conflict types, i.e., SCR (a bicycle crossing the road from right in front of a straight going car) and SSR (a bicycle cut-in from right in front of a straight going car). Either conflict contained various parameterized motion patterns, which were characterized by a combination of parameters: V_c (car velocity), TTC (time-to-collision), V_b (bicycle velocity), and D_{lat} (lateral distance between the car and the bicycle) or V_{lat} (maximum lateral velocity of the bicycle). Some 26 licensed drivers participated in an orthogonal experiment for braking behavior analysis. Results revealed that drivers brake immediately when V-B conflicts occur; hence the BRT (brake reaction time) is independent of any motion pattern parameters. This was further verified by another orthogonal experiment with 10 participants using the eye tracking device. BRT in SSR is longer than that in SCR due to the less perceptible risk and drivers' lower expectation of a collision. The braking intensity and brake Pedal Speed are higher in short-TTC patterns in both conflict types. Therefore, TTC is not a proper activation threshold but a reasonable indicator of braking intensity and Pedal Speed for driver-adaptive AEB systems. By applying the findings in the Bicyclist-AEB, the adaptiveness and acceptability of Bicyclist-AEB systems can be improved.

1. Introduction

Bicycling is an increasingly popular form of daily commute or physical activity [1, 2]. As Vulnerable Road Users (VRU), however, bicyclists are involved in high risk of traffic injuries or fatalities. The NHTSA (National Highway Traffic Safety Administrator) reported that there were nearly 900 yearly bicyclist fatalities in on-road accidents in the US, and this number was reported to be 2440 in the EU [3] and 600 in Japan [4].

Collisions are usually attributed to (1) late brake response and (2) insufficient brake force [5]. Thus, various brake assistance systems were developed to reduce the vehicle-bicycle (V-B) accidents, the Autonomous Emergency Braking (AEB) system, for example. An AEB system is able to actively apply emergency braking if the driver fails to brake in time to avoid a collision. The AEB system for the protection of bicyclists (also called Bicyclist-AEB) is anticipated to be included in the new car safety rating system of the Euro-NCAP (European New Car Assessment Programme) from 2018.

Conventional AEB system estimates the collision risk using the risk metrics such as time-to-collision (TTC) and usually applies a maximum pressure to prevent the collision when TTC is lower than a threshold [6]. Nevertheless, this kind of AEB algorithm is so conservative that it disregards the human factors, which would arouse drivers' distrust and discomfort and even limits the actual effectiveness [7, 8]. One remedy is to adapt the system to human drivers, which requires a throughout investigation on drivers' braking behaviors in V-B conflicts.

Räsänen and Summala [9] investigated the drivers' behaviors in V-B collisions and claimed that the main cause of V-B accidents was drivers' distraction as well as their inappropriate expectation of bicyclists. Wood et al. [10] found that drivers' attitudes regarding bicycle visibility disagree with those of bicyclists, which also causes the V-B accidents. Silvano et al. [11] found that drivers would yield to bicyclists in V-B conflicts at unsignalized roundabouts. Though these researches investigated drivers' behaviors in V-B conflicts, they provided no specific profile of drivers' braking behaviors. Drivers' braking behaviors can be divided into two stages: (1) drivers' prebrake behaviors and (2) postbrake behaviors. The brake reaction time (BRT) is one of the most important metrics characterizing the drivers' prebrake behaviors, defined as the time interval between the occurrence of a stimulus (e.g., sudden intrusion of bicycles) and the pressing on the brake pedal [12]. The auto-brake timing of Bicyclist-AEB can be improved by taking into account the prior knowledge of drivers' BRT. When investigating drivers' postbrake behaviors, braking intensity and brake Pedal Speed are taken into account, characterized as maximum brake pressure, time to maximum brake pressure, vehicle deceleration, and so on [13, 14]. The braking phases of Bicyclist-AEB can be improved by taking into account the prior knowledge of drivers' braking intensity and Pedal Speed.

As suggested by Markkula et al. [15] and Green [16], drivers' braking behaviors are highly dependent on different situations. Summala [17] claimed that drivers' attention is significantly influenced by the environment. For example, complex surrounding traffic is more likely to distract drivers and thus lead to late brake actions. In addition, drivers' anticipation of the potential collisions also significantly affects their response behaviors [9]. It can be deduced that drivers' braking behaviors should also vary in different V-B conflict situations. Hence, it is necessary to categorize the main V-B conflict types and study drivers' braking behaviors in the major conflict types.

Previous studies also found that drivers' braking behaviors vary in different motion patterns of conflicts [13, 14, 18, 19]. This is because drivers' BRT and braking intensity as well as Pedal Speed are strongly dependent on the risk levels, which can be quantified by different motion pattern parameters such as TTC [16], time headways [14], visual looming of the lead vehicle on the driver's retina [13], or other distance-related and velocity-related variables [18, 19]. Chen et al. [20] tackled the effects of the environmental factors on drivers' braking behaviors in V-B conflicts and found that BRT is significantly influenced by visibility, intersection or not, and number of potential threat. However, the conflict scenarios and motion patterns of vehicles and bicycle owe well definition and parameterization in their study. In addition, previous study found that BRT is not a clear value because there is no well-defined indicator to precisely determine the start time of the stimulus [13].

Figure 1: Driving simulator.

Using a driving simulator, however, the V-B conflicts can be triggered in strict accordance with designed conditions by programming. Thus, to study the drivers' braking behaviors in V-B conflicts under different motion patterns, it is necessary to (1) reconstruct the major V-B conflict types by configuring various parameterized motion patterns in driving simulator and (2) study drivers' braking behaviors in V-B conflicts under the corresponding motion patterns.

This study aims to analyze drivers' braking behaviors under different motion patterns of V-B conflicts, for the purpose of improving the design of Bicyclist-AEB systems. Compared with previous field tests, the data in this paper came from simulator tests which are expected to have more reliability. The main contributions of this paper are as follows: (1) the influence of the V-B conflict types and motion patterns on drivers' braking behaviors was calculated; (2) an adaptive Bicyclist-AEB design method considering drivers' braking behaviors was proposed. It should be noted that the methodology and results presented in this paper not only benefit the design of Bicyclist-AEB systems, but also shed light on the improvement of other active safety systems.

The rest of this paper is organized in the following ways: Section 2 introduces the main experiment, including the V-B conflict reconstruction, driving simulator experiment setup, the data processing method, and the results. Section 3 introduces the verification experiment, including experiment details using the eye tracker device and the results. Section 4 discusses the results in Sections 2 and 3 and the improved method about the Bicyclist-AEB design. Section 5 concludes this paper.

2. Main Experiment: Braking Behaviors in Different Motion Patterns

2.1. Apparatus. The experiment was conducted in the driving simulator of Tsinghua University as Figure 1 shows [21]. The driving simulator consists of a visual simulation unit, an audio simulation unit, and a motion simulation unit. The visual simulation was realized by five projected screens: three for front view with a total of 200° field of view and two for rear view with a total of 55° field of view. The audio simulation was realized by a stereo speaker, simulating the various sound of the engine at different rotational speed, the sound of wind, and traffic noises. A real BMW sedan was mounted on a

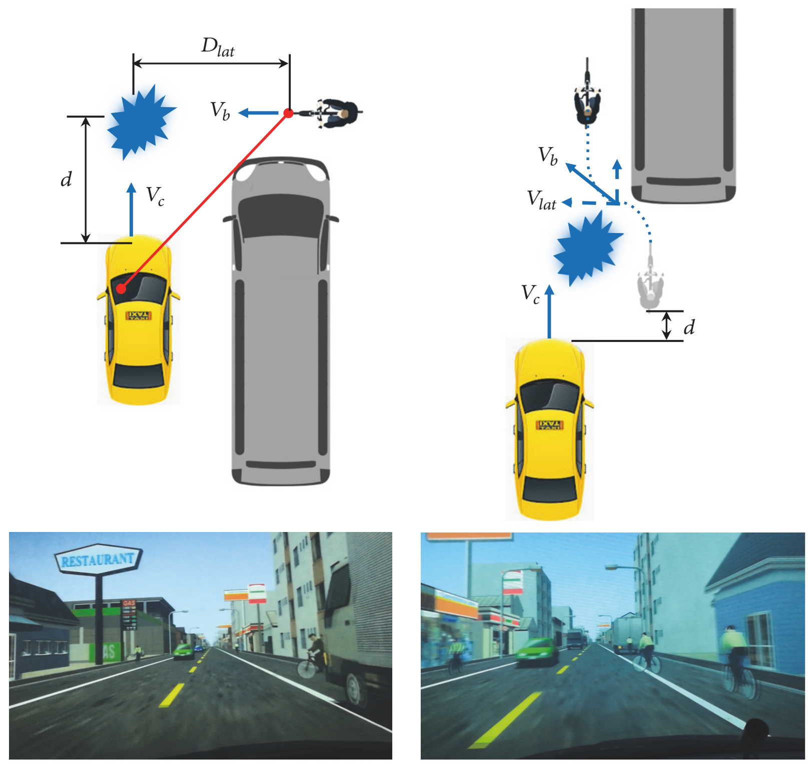

(a) SCR (b) SSR

Figure 2: Reconstruction of typical V-B conflicts and different motion pattern parameters (SCR: bicycle crossing, SSR: bicycle swerving).

six-degree-of-freedom moving base, which provided a ±15° angular and ±0.4m longitudinal moving range. The driving simulator realized the same functions as a real car, including accelerating, steering, and braking, which provided driving experience to participants as realistic as possible. Spatial positions of all the vehicles and bicyclists in the simulation as well as participants' driving performance data (e.g., speed, acceleration, and steering wheel angle) were recorded at 60 Hz.

2.2. Experiment Design

2.2.1. Conflict Reconstruction. Duan et al. [22] investigated V-B accidents in China and categorized V-B conflicts into distinct types based on the relative motion of the vehicle and bicycle and summarized the three most common types: (1) SCR (a bicycle crossing the road from right in front of a straight going car); (2) SCL (a bicycle crossing the road from left in front of a straight going car); (3) SSR (a bicycle cut-in from right in front of a straight going car). Op den Camp et al. [23] and Fredriksson and R. et al. [24] also found that these three types were the major V-B conflict types in Europe. Since there is no significant difference in braking behaviors between SCR and SCL [22], only two typical V-B conflicts (SCR and SSR) were reconstructed in the driving simulator for further study. The reconstruction of the conflict scenario was parameterized with different motion pattern parameters referred to in Green's [16], Matsui et al.'s [19], and Llorca et al.'s [18] researches (see Figure 2). In order to study the relationship between risk degree and braking behavior, it is necessary to trigger bicycle movement under different collision risk degrees. In addition to TTC mentioned above, advanced surrogate safety measures, Time Exposed TTC (TET) and Time Integrated TTC (TIT), were developed based on the TTC notation to access the risks of collisions [25]. However, these two measures usually suffer from the limitation of vehicle trajectories collected over a specific time horizon which are not suitable for this experiment and are not easy to design quantitatively.

The SCR design is shown in Figure 2(a). A bicycle would cross the road at a given constant speed from the right side behind a stopped truck or bus while the ego vehicle was going straight. The movement of the bicycle would be triggered when the instantaneous TTC was below a given threshold. TTC was defined as the collision time if the ego vehicle maintained the current speed. In SCR, TTC was calculated as (1), where V_c was the instantaneous vehicle velocity and d was the longitudinal distance between ego vehicle front end and the bicycle. The position of the bicycle was programmed to ensure that drivers could see the bicycle immediately after the movement was triggered. Oncoming vehicles were presented in the opposite lane to simulate real traffic conditions. Four parameters were defined to describe different motion patterns of SCR, i.e., TTC, vehicle velocity (V_c), bicycle velocity (V_b), and the lateral distance between the right side of ego vehicle and the head of bicycle (D_{lat}). Each parameter was set at three levels (see Table 1).

$$\mathrm{TTC} = \frac{d}{V_c} \tag{1}$$

Table 1: Three-level parameters of different motion patterns.

V_c (km/h)	TTC (s)	V_b (m/s)	D_{lat} (m)	V_{lat} (m/s)
20	1.4	2	1.5	1.2
30	1.7	3	2.0	1.4
40	2.0	4	2.5	1.6

Table 2: Orthogonal experimental setup of SCR.

Group	V_c (km/h)	TTC (s)	V_b (m/s)	D_{lat} (m)
I	20	1.4	2	1.5
	20	1.7	3	2.0
	20	2.0	4	2.5
II	30	1.4	3	2.5
	30	1.7	4	1.5
	30	2.0	2	2.0
III	40	1.4	4	2.0
	40	1.7	2	2.5
	40	2.0	3	1.5

Table 3: Orthogonal experimental setup of SSR.

Group	V_c (km/h)	TTC (s)	V_b (m/s)	V_{lat} (m/s)
I	20	1.4	2	1.2
	20	1.7	3	1.4
	20	2.0	4	1.6
II	30	1.4	3	1.6
	30	1.7	4	1.2
	30	2.0	2	1.4
III	40	1.4	4	1.4
	40	1.7	2	1.6
	40	2.0	3	1.2

The SSR design is shown in Figure 2(b). The ego vehicle was going straight while a bicyclist was riding along the road by the right side at a given constant speed. However, his/her bicycling path was blocked by a stopped vehicle, so he/she cuts into the lane of the ego vehicle without noticing the potential danger. The cut-in movement of the bicycle was triggered when the instantaneous TTC was below a given threshold. In SSR, TTC was defined as (2). Four parameters were defined to describe different motion patterns of SSR, i.e., TTC, vehicle velocity (V_c), bicycle velocity (V_b), and the maximum lateral velocity (V_{lat}). Each parameter was set at three levels (see Table 1).

$$\mathrm{TTC} = \frac{d}{V_c - V_b} \tag{2}$$

2.2.2. Orthogonal Experiment. An orthogonal experiment was designed to analyze drivers' braking behaviors in different motion patterns of SCR and SSR. According to the L9(3^4) orthogonal array, nine combinations of motion patterns were selected for both SCR and SSR, as shown in Tables 2 and 3, respectively.

Then totally 18 conflicts were allocated in an urban traffic environment with signalized intersections as Figure 3 shows. The 18km long two-way one-lane road was divided into three sections (Section 1: 0-6km, Section 2: 6-12km, and Section 3: 12-18km). The 18 conflicts were also divided into three groups by V_c (Group I: 20km/h, Group II: 30km/h, and Group III: 40km/h), and then each group was randomly assigned to one section, as shown in Tables 2 and 3. For each group, 28 parking vehicles (car, truck, or bus) were roughly uniformly allocated along the roadside, among which random six vehicles would be involved with the reconstructed conflicts. The order of conflicts in each group was also random, for the purpose of counterbalancing across participants as well as preventing participants from learning effects.

2.3. Participants. Twenty-six licensed drivers (21 males and 5 females), aging from 22 to 60 years (mean=32.2, SD=9.0), participated in the experiment. Their driving experience varied from 1 to 16 years (mean=6.3, SD=4.3), including not only relatively novice drivers but also quite veteran drivers. However, it was confirmed that all the participants had real-road driving experience for at least 1,000km. Participants included students, officers, workers, and engineers.

2.4. Procedure. Before the experiment, participants were asked to read and sign a statement about the experiment, including an outlook of the experiment and warning of probable discomfort. After a practice driving for 5 minutes, participants continued with the actual experiment if they had adapted to the steering wheel, accelerator pedal, and brake pedal and showed no signs of simulator sickness.

During the experiment, participants were asked to keep their speed around 20, 30, or 40 km/h in each section of the road according to the speed limit sign and drive as they normally would in the real world.

After the experiment, participants were asked to answer a postsimulation questionnaire including the following questions:

Q1. In SCR, you brake immediately or your braking timing depends on your further judgment of situation?

Q2. In SCR, you brake urgently or your brake Pedal Speed depends on your further judgment of situation?

Q3. In SSR, you brake immediately or your braking timing depends on your further judgment of situation?

Q4. In SSR, you brake urgently or your brake Pedal Speed depends on your further judgment of situation?

At last, participants were asked to fill a survey including gender, age, driving experience, level of sickness, and realism for the simulation. The results showed that more than 80% of participants felt a low level of sickness and a high level of realism.

2.5. Results. In total, 468 samples were recorded from the V-B conflicts in experiments, among which 30 samples were discarded because of drivers' sickness of the 3D scenarios in the simulator. Driving performance data of each sample was recorded within a 20s interval (10s before and 10s after the trigger of the bicycle's crossing or cut-in movement). As

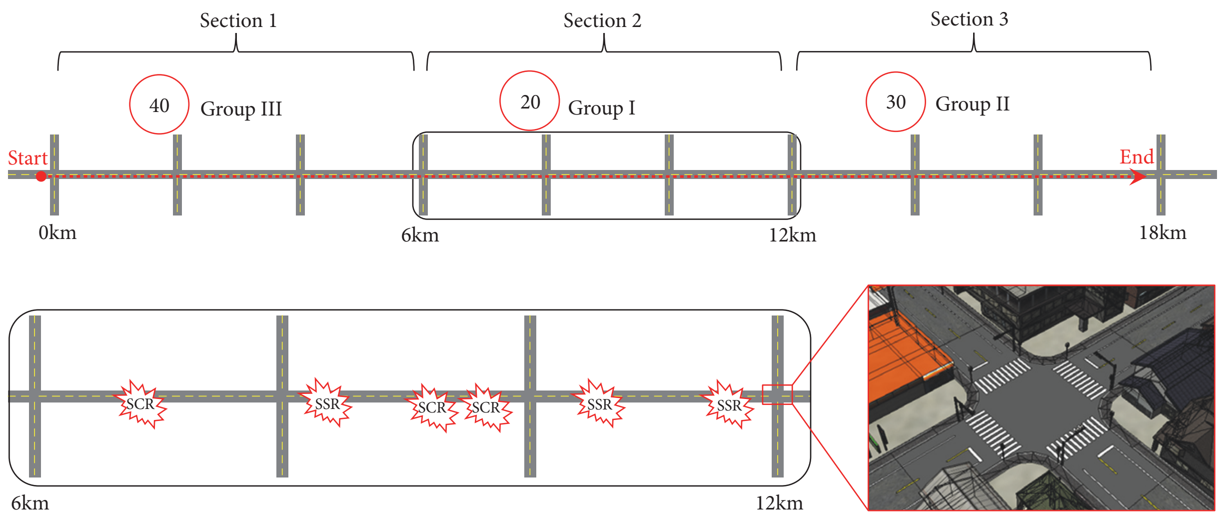

Figure 3: Allocation of the conflicts in simulation.

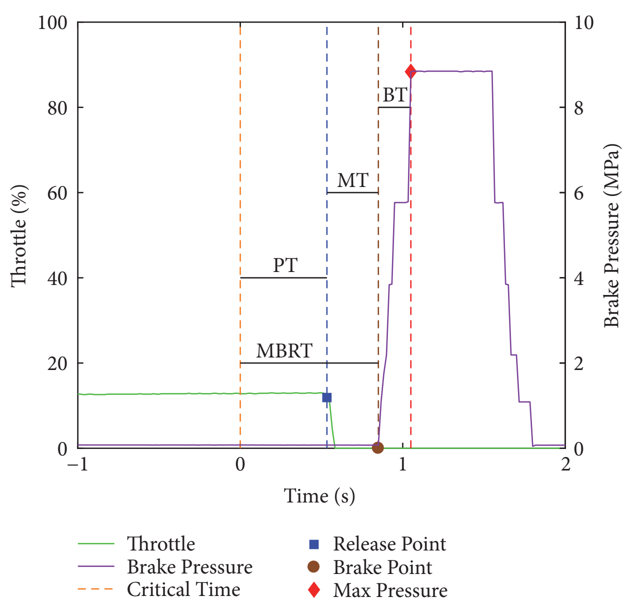

Figure 4: Drivers' braking features in a collision avoidance event sequence.

Figure 4 illustrated, five braking features used in Green's [16] or Wang et al.'s [14] researches were extracted to characterize drivers' braking behaviors in V-B conflicts. The former three (MBRT, PT, and MT) were extracted to investigate drivers' prebrake behaviors, and the other two were extracted to investigate drivers' postbrake behaviors. The feature definitions are given below:

(1) Measured brake reaction time (MBRT): the time interval from the moment when the bicycle's crossing or cut-in movement was triggered (Critical Time in Figure 4) to the moment when the driver pressed the brake pedal (Brake Point in Figure 4).

(2) Perception time (PT): the time interval from Critical Time to the moment when the driver released the accelerator pedal (Release Point in Figure 4).

(3) Movement time (MT): the time interval from Release Point to Brake Point.

(4) Max Pressure: the percent of the maximum brake pressure of the system, which the driver has ever braked up to during the conflict.

(5) Pedal Speed: the mean gradient of brake pressure from Brake Point to the maximum brake pressure point.

The interquartile range along with boxplots was used to detect and discard outliers. Then the missing value was estimated by mean value imputation. The repeated-measures general linear model (GLM) was used to test the statistical significance of braking behaviors' differences in the three levels of each motion parameter. Greenhouse-Geisser correction was applied if the assumption of sphericity of GLM was violated. Bonferroni adjustments were used for post hoc pairwise comparisons of average of each braking feature. The statistical significance level was set at $\alpha = 0.05$.

2.5.1. Measured Brake Reaction Time (MBRT), Perception Time (PT), and Movement Time (MT). Figure 5 shows the average of MBRT, PT, and MT of the drivers in different motion patterns of SCR conflicts. Results show that MBRT is significantly influenced by V_b ($F_{[2,48]} = 19.937$, $p < 0.001$) and D_{lat} ($F_{[2,48]} = 8.057$, $p = 0.001$). PT is significantly influenced by TTC ($F_{[1.508,36.185]} = 5.387$, $p = 0.015$), V_b ($F_{[2,48]} = 7.873$, $p = 0.001$), and D_{lat} ($F_{[2,48]} = 8.069$, $p = 0.001$). In addition, the influence of TTC on MT is significant ($F_{[2,48]} = 21.783$, $p < 0.001$). Post hoc analysis for MBRT, PT, and MT is shown in Table 4.

Figure 6 shows average of MBRT, PT, and MT of the drivers in different motion patterns of SSR conflicts. Results show that MBRT is significantly influenced by V_b ($F_{[2,48]} = 28.067$, $p < 0.001$) and V_{lat} ($F_{[1.442,34.611]} = 65.957$, $p < 0.001$).

Table 4: Post hoc analysis for MBRT, PT, and MT in SCR.

		V_c (km/h)			TTC (s)		
		20 & 30	30 & 40	20 & 40	1.4 & 1.7	1.7 & 2.0	1.4 & 2.0
PT	Difference (s)				0.046	−0.002	0.044
	p-value				**0.005**	0.921	**0.001**
MT	Difference (s)				−0.021	−0.029	−0.050
	p-value				**0.002**	**0.002**	< **0.001**
		V_b (m/s)			D_{lat} (m)		
		2 & 3	3 & 4	2 & 4	1.5 & 2.0	2.0 & 2.5	1.5 & 2.5
MBRT	Difference (s)	0.081	0.062	0.143	−0.057	−0.019	−0.076
	p-value	**0.004**	**0.003**	< **0.001**	**0.001**	0.394	**0.002**
PT	Difference (s)	0.071	0.021	0.092	−0.061	−0.019	−0.080
	p-value	**0.016**	0.386	< **0.001**	**0.003**	0.352	**0.002**

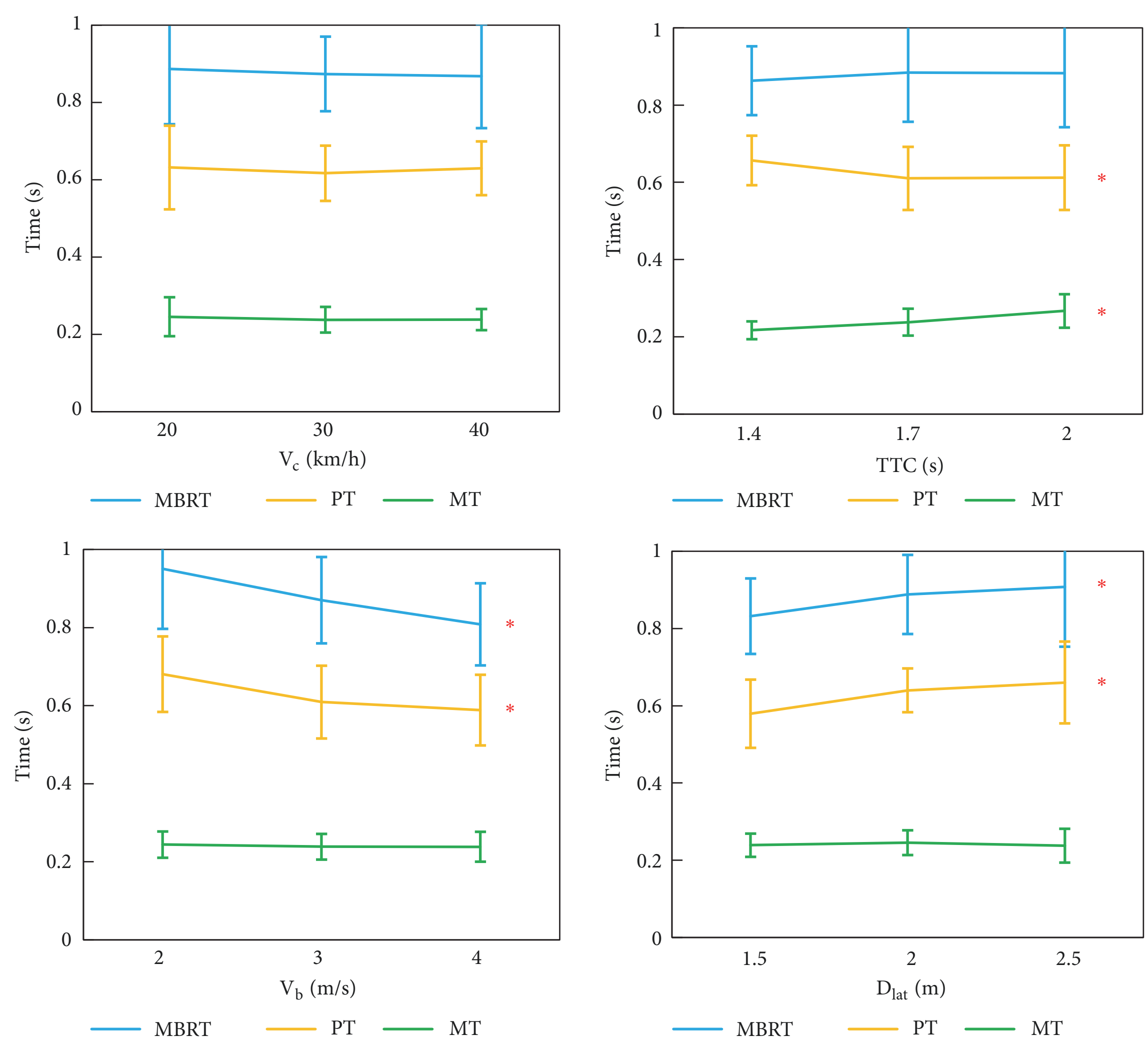

Figure 5: The average (±SD) of MBRT, PT, and MT at three levels of the four parameters in SCR.

PT is significantly influenced by V_b ($F_{[2,48]} = 26.116, p < 0.001$) and D_{lat} ($F_{[2,48]} = 22.834, p < 0.001$). In addition, the influence of TTC ($F_{[2,48]} = 4.554, p = 0.015$) as well as V_b ($F_{[2,48]} = 5.260$, $p = 0.009$) on MT is significant. Post hoc analysis for MBRT, PT, and MT is shown in Table 5.

2.5.2. Max Pressure and Pedal Speed. Figure 7 shows the average of Max Pressure and Pedal Speed in different motion patterns of SCR conflicts. Results reveal a significant influence of TTC on Max Pressure ($F_{[2,48]} = 11.088, p < 0.001$) and Pedal Speed ($F_{[2,48]} = 5.212$, $p = 0.009$. There is a significant

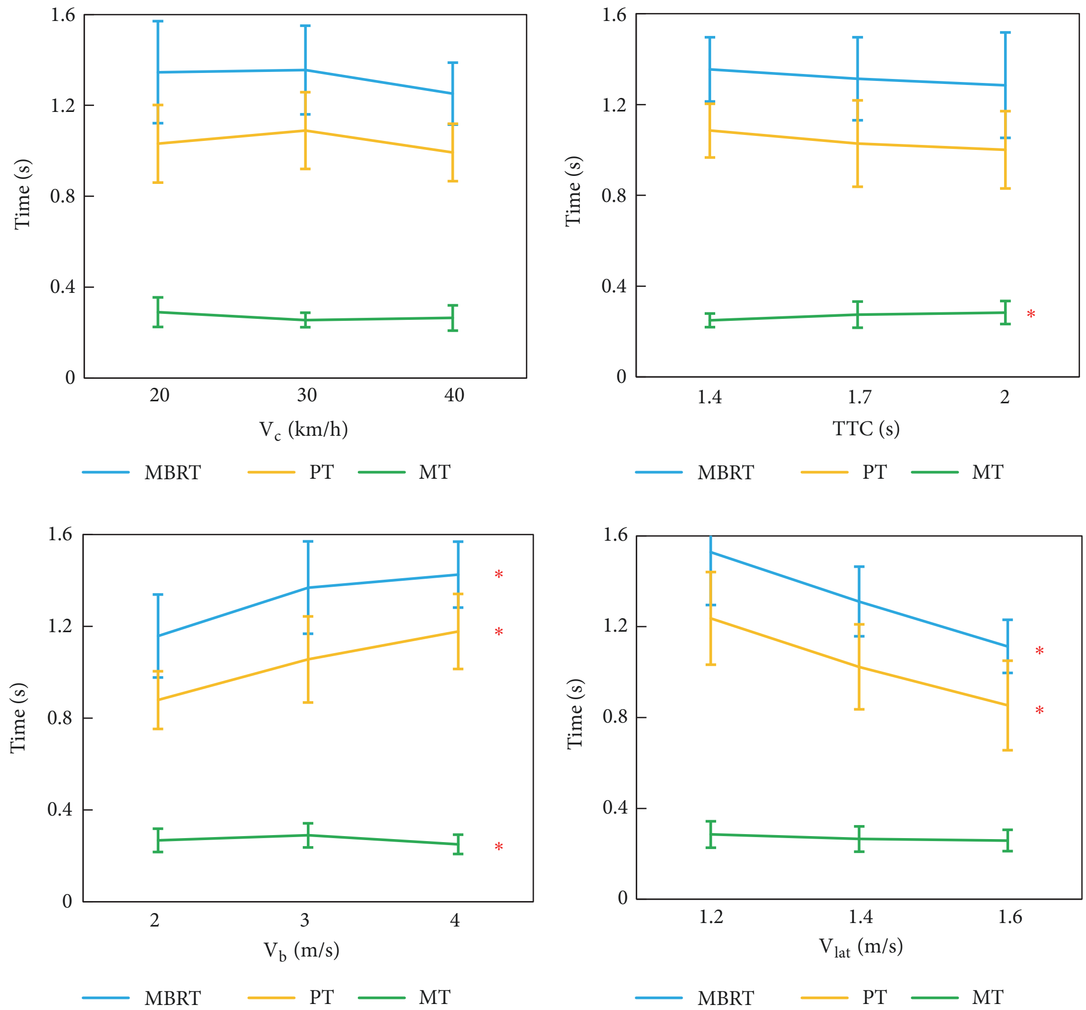

FIGURE 6: The average (±SD) of MBRT, PT, and MT at three levels of the four parameters in SSR.

TABLE 5: Post hoc analysis for MBRT, PT, and MT in SSR.

		V_c (km/h)			TTC (s)		
		20 & 30	30 & 40	20 & 40	1.4 & 1.7	1.7 & 2.0	1.4 & 2.0
MT	Difference (s)				−0.025	−0.009	−0.034
	p-value				0.062	0.474	**0.010**
		V_b (m/s)			V_{lat} (m/s)		
		2 & 3	3 & 4	2 & 4	1.2 & 1.4	1.4 & 1.6	1.2 & 1.6
MBRT	Difference (s)	−0.211	−0.057	−0.268	0.218	0.198	0.416
	p-value	< **0.001**	0.158	< **0.001**	< **0.001**	< **0.001**	< **0.001**
PT	Difference (s)	−0.177	−0.121	−0.298	0.214	0.170	0.384
	p-value	< **0.001**	**0.011**	< **0.001**	**0.002**	**0.002**	< **0.001**
MT	Difference (s)	−0.022	0.039	0.017			
	p-value	0.102	**0.004**	0.129			

influence of V_c ($F_{[2,48]} = 26.116$, $p < 0.001$) and V_b ($F_{[1.419,34.048]} = 28.506$, $p < 0.001$) on Max Pressure. Post hoc analysis for Max Pressure and Pedal Speed is shown in Table 6.

Figure 8 shows the average of Max Pressure and Pedal Speed in different motion patterns of SSR conflicts. Results reveal a significant influence of V_b on Max Pressure ($F_{[2,48]} = 7.478$, $p = 0.001$) and Pedal Speed ($F_{[2,48]} = 4.821$, $p = 0.012$). There is a significant influence of TTC ($F_{[2,48]} = 5.116$, $p = 0.010$) on Pedal Speed. In addition, the influence of V_b ($F_{[2,48]} = 4.233$, $p = 0.020$) as well as V_{lat} ($F_{[1.562,37.486]} = 18.752$, $p < 0.001$) on Max Pressure is significant. Post hoc analysis for Max Pressure and Pedal Speed is shown in Table 7.

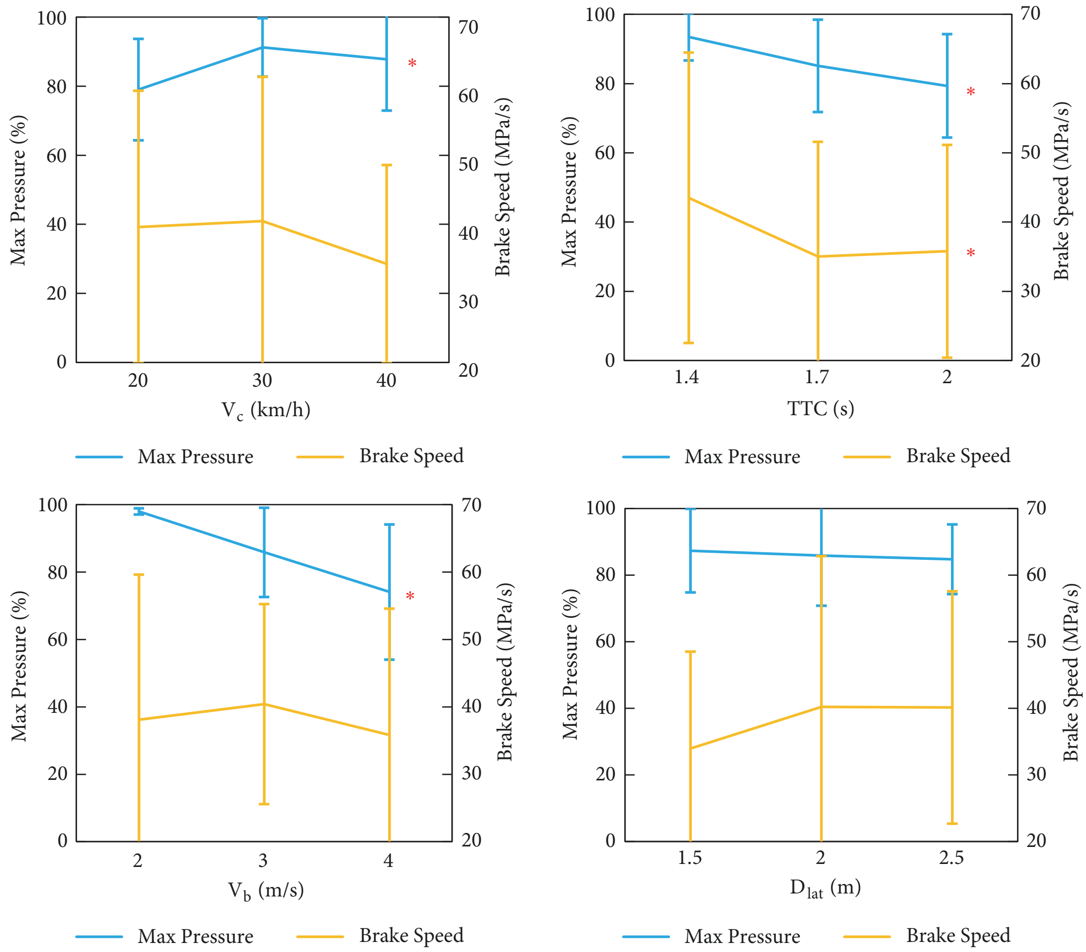

Figure 7: The average (±SD) of Max Pressure and Pedal Speed at three levels of the four parameters in SCR.

Table 6: Post hoc analysis for Max Pressure and Pedal Speed in SCR.

			V_c (km/h)			TTC (s)	
		20 & 30	30 & 40	20 & 40	1.4 & 1.7	1.7 & 2.0	1.4 & 2.0
Max Pressure	Difference (%)	−12.233	3.427	−8.806	8.420	5.747	14.167
	p-value	< **0.001**	0.161	**0.010**	< **0.001**	**0.018**	< **0.001**
Pedal Speed	Difference (MPa/s)				8.478	−0.757	7.721
	p-value				**0.002**	0.797	**0.029**
			V_b (m/s)			D_{lat} (m)	
		2 & 3	3 & 4	2 & 4	1.5 & 2.0	2.0 & 2.5	1.5 & 2.5
Max Pressure	Difference (%)	12.147	11.767	23.9			
	p-value	< **0.001**	< **0.001**	< **0.001**			

2.5.3. Comparison of SCR and SSR. Table 8 summarized the drivers' braking behaviors in SCR and SSR conflicts. Student's t-test revealed that the difference of the former four features (MBRT, PT, MT, and Max Pressure) between SCR and SSR is significant while there is no significant difference of Pedal Speed between SCR and SSR.

Table 9 shows participants' answer to the four questions in Section 2.3. Q1 and Q3 subjectively investigate drivers' prebrake behaviors while Q2 and Q4 for postbrake behaviors. Fisher exact test result reveals that there is no significant difference of prebrake behaviors or postbrake behaviors between SCR and SSR conflicts.

3. Verification Experiment: Evolutionary Process of the Stimulus in Different Motion Patterns

Given the results in Section 2.5.1, for most cases, drivers' MBRT and PT do not vary significantly with different V_c

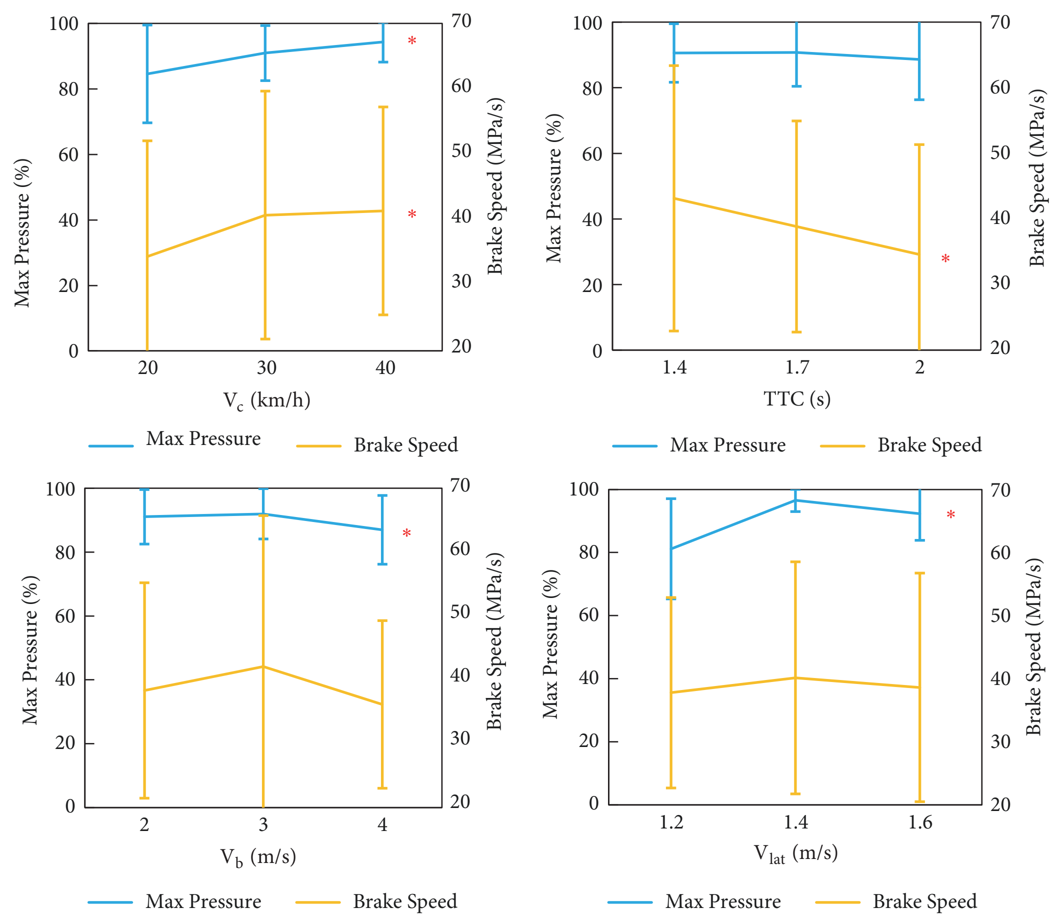

FIGURE 8: The average (±SD) of Max Pressure and Pedal Speed at three levels of the four parameters in SSR.

TABLE 7: Post hoc analysis for Max Pressure and Pedal Speed in SSR.

		V_c (km/h)			TTC (s)		
		20 & 30	30 & 40	20 & 40	1.4 & 1.7	1.7 & 2.0	1.4 & 2.0
Max Pressure	Difference (%)	−6.334	−3.400	−9.734			
	p-value	**0.042**	0.090	**0.001**			
Pedal Speed	Difference (MPa/s)	−6.324	−0.641	−6.965	4.299	4.267	8.566
	p-value	**0.031**	0.766	**0.011**	0.196	0.097	**0.001**
		V_b (m/s)			V_{lat} (m/s)		
		2 & 3	3 & 4	2 & 4	1.2 & 1.4	1.4 & 1.6	1.2 & 1.6
Max Pressure	Difference (%)	−0.862	4.960	4.097	−15.367	4.211	−11.155
	p-value	0.632	**0.008**	**0.046**	< **0.001**	**0.026**	**0.001**

TABLE 8: Summary of drivers' braking features in SCR and SSR conflicts.

	SCR		SSR		Difference
	Average	SD	Average	SD	
MBRT (s)	0.88	0.17	1.32	0.34	−0.44*
PT (s)	0.63	0.14	1.04	0.34	−0.41*
MT (s)	0.24	0.06	0.27	0.09	−0.03*
Max Pressure (%)	86.0	22.2	91.8	15.5	−5.9*
Pedal Speed (MPa/s)	38.1	24.9	38.9	22.4	−0.7

*Significant at α=0.05.

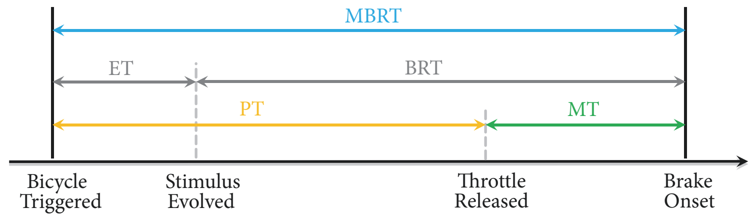

Figure 9: Segmentation of drivers' prebrake behavior sequence.

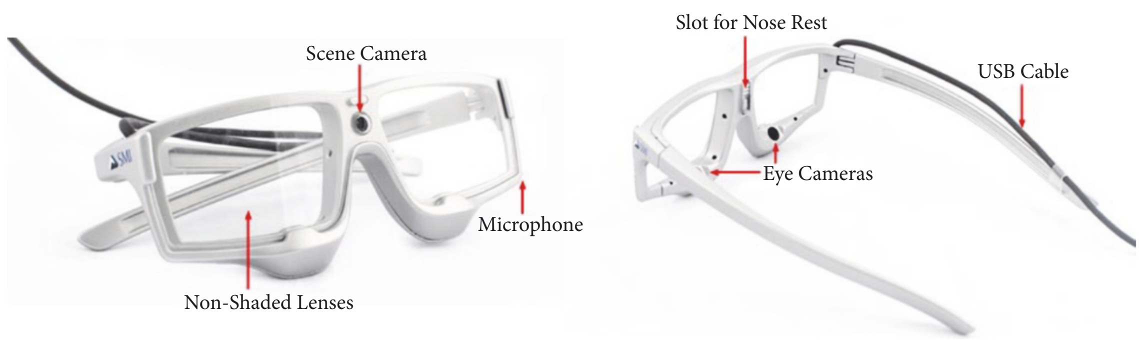

Figure 10: Eye tracking device.

Table 9: Summary of drivers' answers to postsimulation questionnaire.

Braking intention		SCR	SSR
Pre-brake	Brake immediately	20	15
	Not definitely immediately	5	10
Post-brake	Brake urgently	18	15
	Not definitely urgently	7	10

or TTC. Hence, we can infer that drivers always brake without hesitation in this emergency, regardless of the motion patterns (we call it pattern-independent). The postsimulation questionnaire result that most of drivers choose braking immediately in both SCR and SSR conflicts (see Table 9) confirms this inference from a subjective aspect.

However, some results contradict the above conclusion. More exactly, MBRT and PT are significantly dependent on motion pattern parameter V_b as well as D_{lat} in SCR and V_b as well as V_{lat} in SSR (we call it pattern-dependent). We speculate that this may be due to our definition of the brake reaction time.

In the experiment mentioned above, the start of the brake reaction time is defined as the moment when the bicycle is triggered by programming, which is called measured brake reaction time (MBRT). Although the MBRT is easily measured and is of reliable accuracy, drivers cannot recognize its start time immediately. Markkula et al. [13] indicated that drivers' braking reaction should not be thought as a reaction to the researcher-defined "hazard onset" but instead as a reaction to the visual looming cues that build up later on in the evolving traffic scenario. Likewise, the brake reaction time (BRT) is computed from the start of stimulus according to the definition presented by SAE [12]. Hence, the BRT should start from the moment when the intrusive bicycle has evolved into a stimulus instead of the moment when the bicycle is triggered, as Figure 9 shows. It is clear that there is a time interval between these two moments, which is referred to as evolving time (ET).

In summary, we infer that MBRT and PT are exceptionally pattern-dependent because both MBRT and PT contain ET. In other words, the BRT should be independent of all the four motion parameters, although MBRT is not. An experiment was designed to verify this assumption and then objectively confirm the inference that drivers always tend to brake without hesitation in emergency. For this purpose, it is necessary to determine the moment when the intrusive bicycle has evolved into a stimulus and then decompose MBRT into ET and BRT for further analyses.

3.1. Apparatus and Experiment Design. The experiment was conducted under the same driving simulator as in Section 2.1 and the same experiment conditions as in Section 2.2. Besides, the SMI Eye Tracking Glasses (ETG) 2w were used to capture drivers' eye movements with a 60Hz binocular sampling rate as Figure 10 shows. The ETG were worn as a normal pair of glasses and connected to a recording device. This device should be initialized by using the one-point calibration method before the experiment. Two small cameras on the bottom rim of the glasses captured the eye movements of the driver and mapped the driver's gaze point into a scene video. The gaze tracking range of the ETG was 80° horizontally and 60° vertically. The gaze position accuracy of the ETG was 0.5° over all distances.

3.2. Participants and Procedure. Ten licensed drivers (7 males and 3 females), aging from 24 to 53 years (mean=33.2,

Table 10: Post hoc analysis for MBRT and ET in SCR.

		V_b (m/s)			D_{lat} (m)		
		2 & 3	3 & 4	2 & 4	1.5 & 2.0	2.0 & 2.5	1.5 & 2.5
MBRT	Difference (s)	0.019	0.055	0.074	−0.058	−0.012	−0.070
	p-value	1.000	0.129	**0.012**	0.088	1.000	0.091
ET	Difference (s)	0.063	0.018	0.081	−0.072	−0.033	−0.104
	p-value	**0.030**	0.934	**0.043**	0.070	0.908	0.121

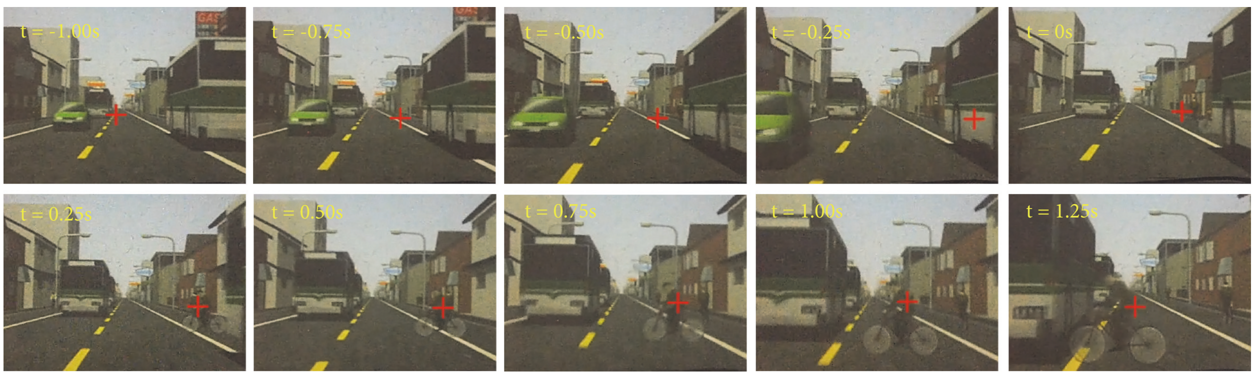

Figure 11: Part of the scene frames captured by the ETG (the red cross indicated the driver's gaze point). t = 0s is the moment of the bicycle triggering. t = 0.25s is the moment when the driver started gazing at the bicycle, i.e., the moment when the stimulus was established.

SD=8.5), whose driving experience varied from 3 to 15 years (Mean=7.2, SD=3.4) participated in the experiment. The experiment procedure was the same as Section 2.4 except that drivers were not asked to answer the questionnaire.

3.3. Results. In total, 180 samples were recorded from the V-B conflicts in experiments, among which 11 samples were discarded because of drivers' sickness of the 3D scenarios in the simulator. MBRT was extracted from the driving performance data as Figure 4 shows. As Figure 11 shows, the driver scanned the vehicles, bicycles, or other interesting objects/area before a V-B conflict occurred while gazing at the intrusive bicycle after the conflict occurred. The moment when the driver started gazing at the bicycle was determined as the moment when the stimulus was established in a V-B conflict. Then ET and BRT were extracted from the driving performance data and the eye movement data. The data processing method was the same as Section 2.5.

3.3.1. Measured Brake Reaction Time (MBRT), Evolving Time (ET), and Brake Reaction Time (BRT). Figure 12 shows average of MBRT, ET, and BRT of the drivers in different motion patterns of SCR conflicts. Results show that there is no significant influence of V_c ($F_{[2,18]} = 2.027$, $p = 0.161$), TTC ($F_{[1.270,11.426]} = 1.766$, $p = 0.214$), V_b ($F_{[2,18]} = 0.488$, $p = 0.622$), or D_{lat} ($F_{[2,18]} = 0.260$, $p = 0.774$) on BRT. MBRT is significantly influenced by V_b ($F_{[2,18]} = 6.120$, $p = 0.009$) and D_{lat} ($F_{[1.300,11.696]} = 5.996$, $p = 0.025$). ET is significantly influenced by V_b ($F_{[2,18]} = 7.898$, $p = 0.003$) and D_{lat} ($F_{[2,18]} = 4.911$, $p = 0.020$). Post hoc analysis for MBRT and ET is shown in Table 10.

Figure 13 shows average of MBRT, ET, and BRT of the drivers in different motion patterns of SSR conflicts. Results show that there is no significant influence of V_c ($F_{[2,18]} = 0.046$, $p = 0.955$), TTC ($F_{[2,18]} = 0.947$, $p = 0.406$), V_b ($F_{[2,18]} = 1.137$, $p = 0.343$), or V_{lat} ($F_{[2,18]} = 0.592$, $p = 0.563$) on BRT. MBRT is significantly influenced by V_b ($F_{[2,18]} = 13.249$, $p < 0.001$) and V_{lat} ($F_{[2,18]} = 13.296$, $p < 0.001$). ET is significantly influenced by V_b ($F_{[2,18]} = 6.413$, $p = 0.008$) and V_{lat} ($F_{[1.244,11.193]} = 9.835$, $p = 0.007$). Post hoc analysis for MBRT and ET is shown in Table 11.

3.3.2. Comparison of SCR and SSR. Table 12 summarized the drivers' braking behaviors in SCR and SSR conflicts. Student's t-test revealed that the difference of MBRT, ET, and BRT between SCR and SSR is significant.

4. Discussion

4.1. Prebrake Behaviors. As mentioned above, we subjectively infer from the results in Section 2.5.3 that drivers always brake without hesitation in such emergency, regardless of the motion patterns (pattern-independent). While most of the results in Section 2.5.1 objectively support our speculation, some exceptions seem to contradict the inference. More exactly, MBRT and PT are significantly dependent on V_b as well as D_{lat} in SCR and V_b as well as V_{lat} in SSR (pattern-dependent). According to the results of verification experiment in Section 3.3.1, this is due to the different ET in different level of V_b and D_{lat} or V_{lat}. Specifically, in SCR conflicts, the crossing bicycle does not evolve into a stimulus until it intrudes into the driver's attention view. As Figures 14(a) and 14(b) illustrated, the bicycle intrudes into

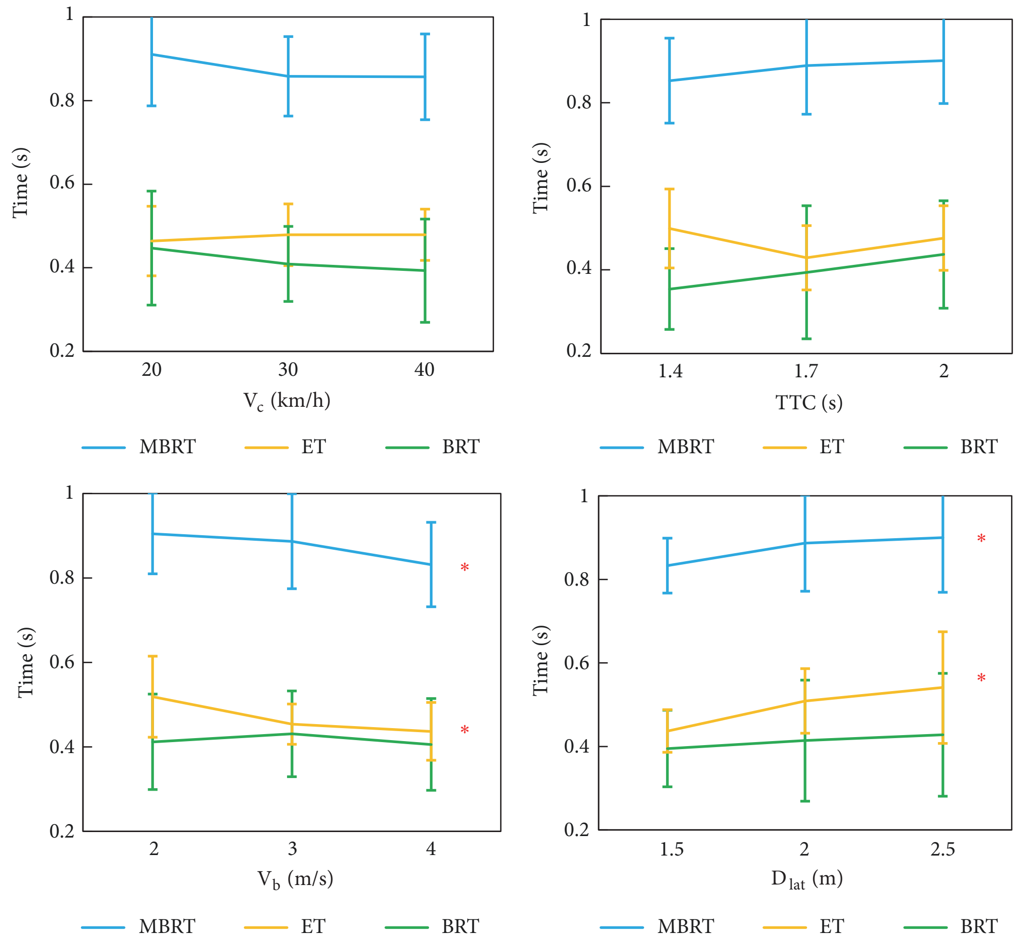

Figure 12: The average (±SD) of MBRT, ET, and BRT at three levels of the four parameters in SCR.

Table 11: Post hoc analysis for MBRT and ET in SSR.

		V_b (m/s)			V_{lat} (m/s)		
		2 & 3	3 & 4	2 & 4	1.2 & 1.4	1.4 & 1.6	1.2 & 1.6
MBRT	Difference (s)	−0.204	−0.033	−0.236	0.099	0.255	0.354
	p-value	< **0.001**	1.000	**0.007**	0.708	**0.021**	**0.001**
ET	Difference (s)	−0.314	0.081	−0.233	0.123	0.260	0.383
	p-value	**0.001**	1.000	0.172	0.967	**0.016**	**0.001**

Table 12: Summary of drivers' braking features in SCR and SSR conflicts.

	SCR		SSR		Difference
	Average	SD	Average	SD	
MBRT (s)	0.88	0.14	1.31	0.30	−0.43*
ET (s)	0.47	0.12	0.82	0.35	−0.36*
BRT (s)	0.41	0.15	0.49	0.21	−0.08*

*Significant at α=0.05.

the driver's attention view earlier with rising V_b and declining D_{lat}, which leads to a shorter ET (see Figure 12). In the context that drivers always brake immediately in emergency, shorter ET then leads to shorter PT and MBRT. Similarly, in SSR conflicts, the preceding bicycle is not a stimulus at the beginning of the cut-in movement until it has turned a considerable angle. As Figures 14(c) and 14(d) illustrated, bicycle's turning angle increases with rising V_{lat} and declining V_b, which means that the bicycle evolves into a stimulus earlier, resulting in shorter ET (see Figure 13), then leading to shorter PT and MBRT. In a word, it is the time difference between MBRT and BRT, i.e., ET, that contributes to the variation of MBRT in different level of V_b and D_{lat} or V_{lat}.

Combining the results of the main experiment in Section 2.5.1 with the results of the verification experiment in Section 3.3.1, we can draw a conclusion that drivers' BRT is independent of any of the four motion pattern parameters, which confirms the inference that drivers always tend to brake without hesitation in emergency from an objective

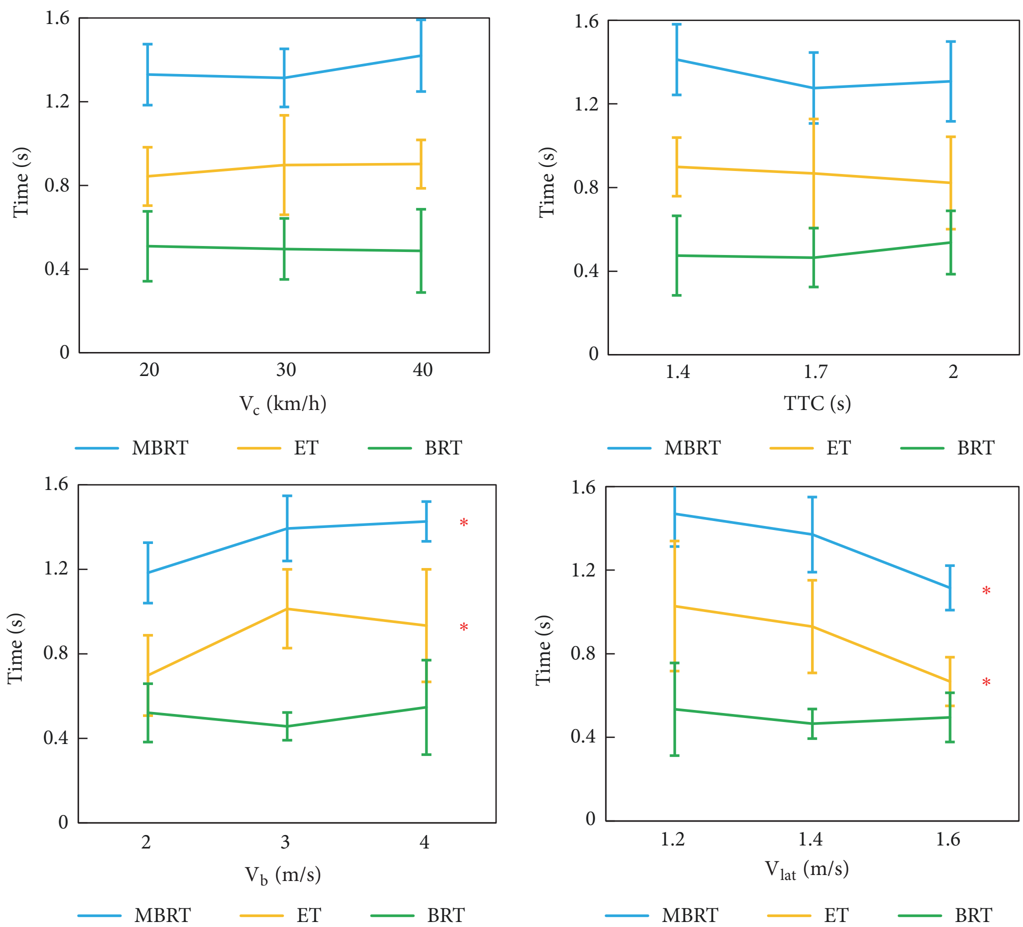

Figure 13: The average (±SD) of MBRT, ET, and BRT at three levels of the four parameters in SSR.

aspect. This finding reveals that TTC may not be a reasonable threshold for the activation of AEB system because drivers would brake immediately rather than at certain TTC in V-B conflicts.

In addition, though MT is observed to be pattern-dependent under certain combinations of motion pattern parameters, the variation is always less than 0.02s, which is close to the sampling precision of the driving simulator (1/60s). It means that MT is more like a fixed value in different motion patterns, which is consistent with the finding of Wang et al. [14] that neither time headway nor lead vehicle deceleration affects MT in rear-end conflicts.

Comparing the results in two conflict types, MBRT (and BRT), PT and ET are significantly longer in SSR than in SCR (we call it type-dependent) because the evolution of the stimulus is much slower in a cut-in movement than in an abrupt lateral crossing from behind the obstruction. MT is also significantly longer in SSR than in SCR, which indicates that drivers have a longer brake delay in SSR. This is because, in SSR, drivers will hesitate to brake when they expect the bicyclist to be aware of the risk and swerve back to bicycle track. However, in SCR, drivers do not have such expectation. These intertype differences are consistent with the results of our previous research [22].

4.2. Postbrake Behaviors. Max Pressure and Pedal Speed were used to analyze postbrake behaviors which imply the drivers' subjective perceived risk in V-B conflicts [14]. Given the results in Section 2.5.2, Max Pressure and Pedal Speed have a similar tendency with respect to almost all motion pattern parameters. Specifically, both are negatively correlated with TTC (i.e., TTC-dependent). In other words, drivers intend to brake harder and more urgently in short-TTC scenarios due to the higher risk perceived subjectively by the driver. This phenomenon also demonstrates the rationality of the common usage of TTC as a risk assessment indicator for intelligent vehicles [26].

However, there are some exceptions to the similar tendency mentioned above. In SSR conflicts, Max Pressure remains high no matter how TTC changes, since the bicycle is always in a hazardous area ahead of the ego vehicle (see Figure 15(b)) till it swerves back to bicycle track. Therefore, drivers must stop the vehicle with a high braking intensity no matter how large the TTC is. In SCR, however, the bicycle just passes through the hazardous area rather than staying in it (see Figure 15(a)). Specifically, in high-V_b cases, the bicycle has passed through the hazardous area before the driver presses the brake pedal to reach a high braking intensity. This may explain why drivers felt more hazardous and braked

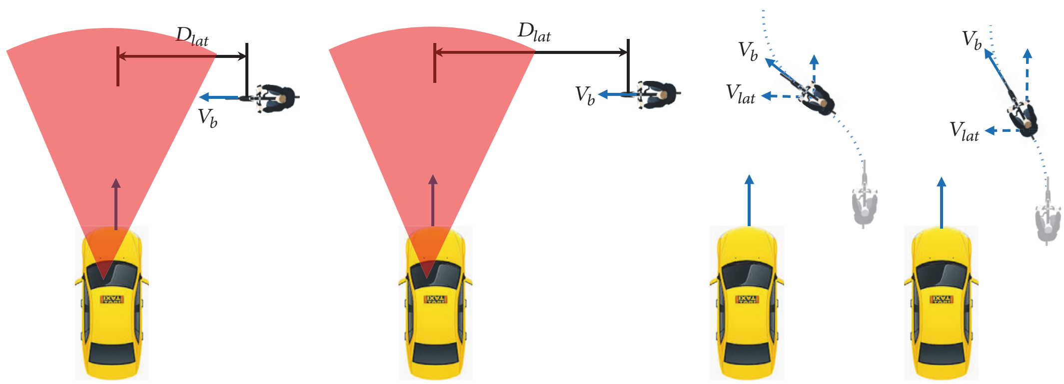

(a) Short D_{lat} and high V_b, SCR (b) Long D_{lat} and low V_b, SCR (c) High V_{lat} and low V_b, SSR (d) Low V_{lat} and high V_b, SSR

Figure 14: The influence of V_b and D_{lat} or V_{lat} on ET.

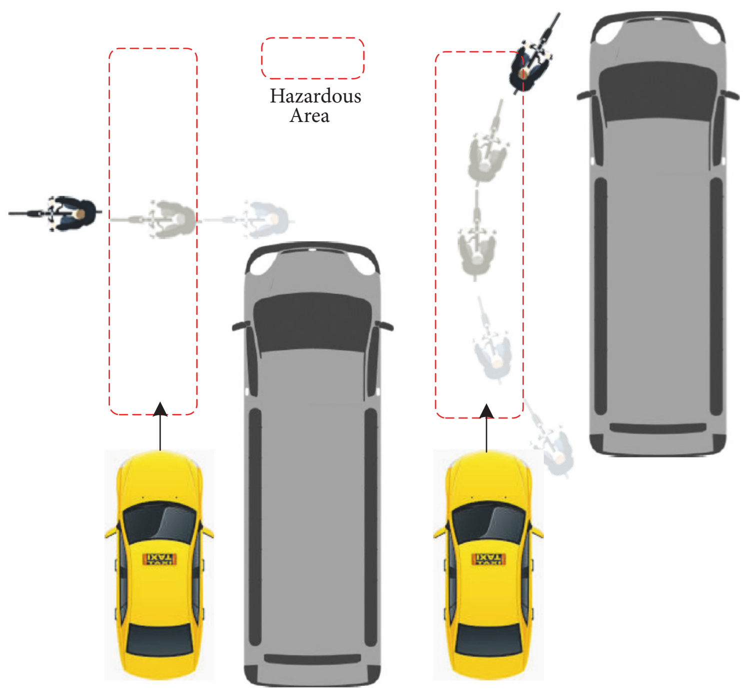

(a) SCR (b) SSR

Figure 15: The hazardous area in SCR and SSR conflicts.

harder when V_b was low. This is consistent with the finding of Markkula et al. [13] that the maximum deceleration of ego vehicle varies with motion patterns in rear-end near-crashes because drivers will not continue to brake harder once the collision is avoided.

Furthermore, the result that Max Pressure is significantly higher in SSR than in SCR (type-dependent) can also be explained by the different hazardous area mentioned above. But the difference of Pedal Speed is not significant between SSR and SCR conflicts (type-independent), which is consistent with the postsimulation questionnaire results that most of drivers choose braking urgently in both SCR and SSR conflicts (see Table 9).

4.3. Guidelines for the Development of Bicyclist-AEB. Conventional AEB systems are usually activated by a TTC threshold (denoted as TTC_b) and then apply a step brake pressure from zero to the ultimate maximum to avoid or mitigate collision [6]. Here TTC_b is usually calculated when assuming an ultimate deceleration at the current relative distance and velocity. Such conservative strategy can avoid collisions and reduce drivers' annoyance when drivers' reaction to the emergency is unknown. Nevertheless, this activation timing could be too late if compared with drivers' BRT and the step brake phase could be too urgent if compared with drivers' postbrake behaviors, both of which may result in drivers' distrust and restrict the effect of Bicyclist-AEB. A clear

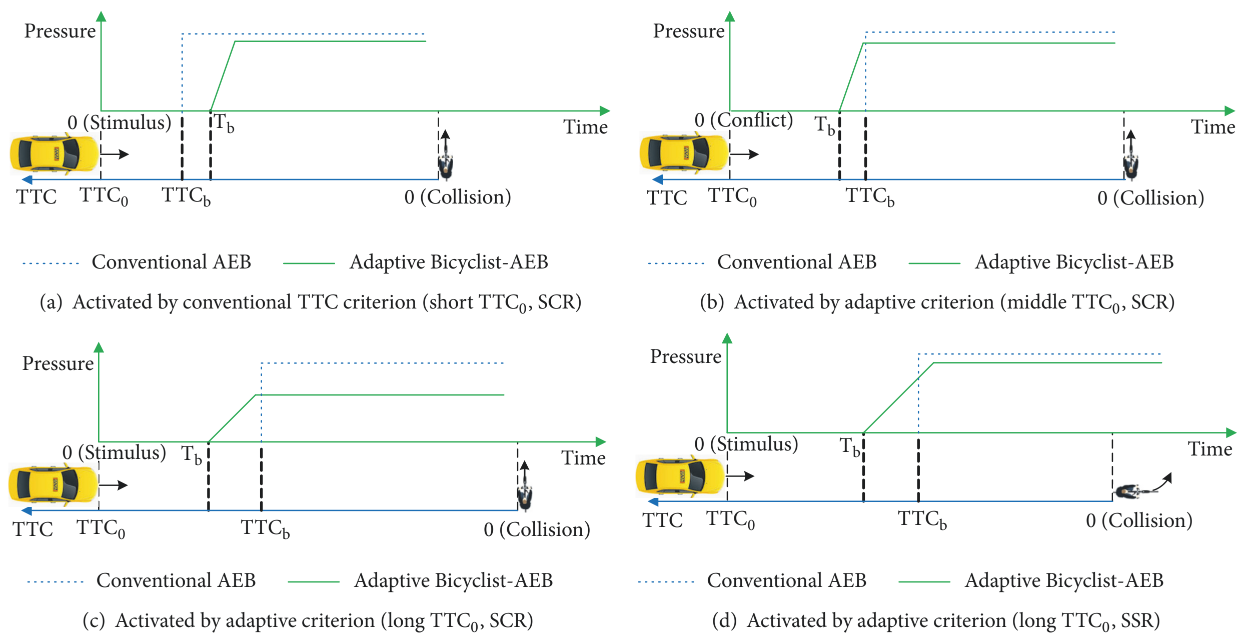

(a) Activated by conventional TTC criterion (short TTC_0, SCR)

(b) Activated by adaptive criterion (middle TTC_0, SCR)

(c) Activated by adaptive criterion (long TTC_0, SCR)

(d) Activated by adaptive criterion (long TTC_0, SSR)

Figure 16: Comparison between conventional AEB and adaptive Bicyclist-AEB on activation timing and brake phases.

understanding of driver responses to various V-B conflict situations would significantly improve the performance of Bicyclist-AEB system.

Given the results of drivers' prebrake behaviors mentioned above, a new activation criterion is proposed to improve the auto-brake timing of Bicyclist-AEB systems. The new criterion is denoted as T_b, which is typically defined as drivers' average BRT in SCR or SSR conflicts. The auto-brake activation condition is $T \geq T_b$, where T is computed from the start of the stimulus. T_b can be also chosen as some percentile of the observed BRTs according to the designer's preference. A longer T_b indicates a more conservative strategy. Given the results of drivers' postbrake behaviors, a new braking intensity and Pedal Speed criterion is proposed to improve the braking phases of automatic braking. The new criterion replaces the step brake pressure of conventional AEB with a ramp brake pressure, whose gradient and terminal are, respectively, defined as drivers' average Pedal Speed and Max Pressure with respect to the instantaneous TTC at the start of the stimulus, which is denoted as TTC_0.

For practical applications, a Bicyclist-AEB system would continuously monitor the TTC and T after the occurrence of the crossing or cut-in bicycle and compare them with the corresponding TTC_b and T_b, respectively. If the TTC criterion is met first, the AEB will be activated by $TTC \leq TTC_b$ and a step brake pressure will be applied to avoid forward collisions which is actually the conventional AEB strategy. As Figure 16(a) shows, for example, in a SCR conflict with short TTC_0, it would be too late to activate the AEB by the condition $T \geq T_b$. In such extremely emergency case, it is more crucial to ensure the avoidance than to consider drivers' reaction, which means that the activation and braking phases are irrelevant to the current conflict type or motion pattern. While in cases, where TTC_0 is longer, the condition $T \geq T_b$ is met first, then the proposed adaptive Bicyclist-AEB will be activated instead, as Figures 16(b)–16(d) shows. The activation is relevant to the conflict type, and the braking intensity as well as Pedal Speed is relevant to TTC_0. More specifically, comparing Figure 16(b) with Figure 16(c), where the only difference is TTC_0, the activation timing is the same since BRT is TTC-independent, but Max Pressure and Pedal Speed are higher in Figure 16(c) because they are negatively correlated with TTC (See Figure 7). Comparing Figure 16(c) with Figure 16(d), where the only difference is the conflict type, T_b is longer in Figure 16(d) because drivers' BRT in SCR is supposed to be shorter than that in SSR, while Pedal Speed is the same since it is type-independent (See Table 8). Note that Max Pressure is higher in Figure 16(d) due to the wide hazardous area in SSR (see Figure 15(b)).

5. Conclusion

In this paper, the two most typical V-B (vehicle-bicycle) conflicts were extracted to be studied according to previous studies. They were SCR (a bicycle crossing the road from right in front of a straight going car) and SSR (a bicycle cut-in from right in front of a straight going car). A high fidelity driving simulator was used to investigate drivers' braking behaviors in both types under parameterized motion patterns which were described by V_c (car velocity), TTC (time-to-collision), V_b (bicycle velocity), and D_{lat} (lateral distance between the car and the bicycle) or V_{lat} (maximum lateral velocity of the bicycle). An eye tracking device was used to investigate the evolutionary process of the stimulus in V-B conflicts. The influence of motion patterns on drivers' both prebrake and postbrake behaviors was analyzed through an orthogonal experiment. Results revealed that drivers brake immediately when V-B conflicts occur; hence the BRT is independent of any motion pattern parameters. But BRT in SSR is longer than that in SCR due to the less perceptible risk and drivers' lower expectation of a collision. Both braking intensity and brake Pedal Speed are higher in short-TTC patterns in both conflict types. Therefore, TTC is not a proper activation threshold but a reasonable indicator of braking intensity and Pedal Speed for driver-adaptive AEB systems.

Given the results, a method to improve the auto-brake timing and braking phases of an adaptive Bicyclist-AEB system was proposed in this paper. This method takes into account drivers' prebrake behaviors and postbrake behaviors in different motion patterns of V-B conflicts to improve the AEB activation conditions and braking phases. Such adaptive brake timing and braking phases may increase drivers' acceptance of AEB systems.

In the future, we will examine whether driver properties, traffic environment, and road alignment would influence the braking behavior in different V-B conflicts.

Data Availability

The data used to support the findings of this study are available from the corresponding author upon request.

Disclosure

This study was based on our previous oral presentation titled "Drivers' Braking Behaviors in Different Motion Patterns of Vehicle-Bicycle Conflicts" in the FAST-zero'17 symposium, Nara, Japan, 2017.

Conflicts of Interest

The authors declare that they have no conflicts of interest.

Authors' Contributions

Lian Hou and Jingliang Duan have equally contributed to this research work.

Acknowledgments

This study was supported by Toyota Motor Corporation and Chinese government (Grant Nos. 2016YFB0100906, 2016YFE0102200, and 2017YFC0803802) and NSF China (Grant no. 51805332). We would like to acknowledge them for funds that made this project possible.

References

[1] E. Heinen, K. Maat, B. Wee, and Van., "The role of attitudes toward characteristics of bicycle commuting on the choice to cycle to work over various distances," *Transportation Research Part D*, vol. 16, pp. 102–109, 2011.

[2] J. Pucher, R. Buehler, and M. Seinen, "Bicycling renaissance in North America? An update and re-appraisal of cycling trends and policies," *Transp. Res. Part A*, vol. 45, pp. 451–475, 2011.

[3] N. Marković, D. R. Pešić, B. Antić, and M. Vujanić, "The analysis of influence of individual and environmental factors on 2-wheeled users' injuries," *Traffic Injury Prevention*, vol. 17, pp. 610–617, 2016.

[4] Y. Matsui and S. Oikawa, "Risks of serious injuries and fatalities of cyclists associated with impact velocities of cars in car-cyclist accidents in Japan," *Stapp Car Crash Journal*, vol. 59, pp. 385–400, 2015.

[5] S. O. Y. Sohn and R. Stepleman, "Meta-analysis on total braking time," *Ergonomics*, vol. 41, pp. 1129–1140, 2017.

[6] K. D. Kusano and H. C. Gabler, "Safety benefits of forward collision warning, brake assist, and autonomous braking systems in rear-end collisions," *IEEE Transactions on Intelligent Transportation Systems*, vol. 13, pp. 1546–1555, 2012.

[7] A. H. Eichelberger and A. T. Mccartt, "Volvo drivers' experiences with advanced crash avoidance and related technologies volvo drivers ' experiences with advanced crash avoidance and related technologies," *Traffic Injury Prevention*, vol. 15, pp. 187–195, 2014.

[8] B. Fildes, M. Keall, N. Bos et al., "Effectiveness of low speed autonomous emergency braking in real-world rear-end crashes," *Accident Analysis & Prevention*, vol. 81, pp. 24–29, 2015.

[9] M. Räsänen and H. Summala, "Attention and expectation problems in bicycle – car collisions: an in-depth study," *Accident Analysis & Prevention*, vol. 30, pp. 657–666, 1998.

[10] J. M. Wood, P. F. Lacherez, R. P. Marszalek, and M. J. King, "Drivers' and cyclists' experiences of sharing the road: incidents, attitudes and perceptions of visibility," *Accident Analysis & Prevention*, vol. 41, pp. 772–776, 2009.

[11] A. P. Silvano, X. Ma, and H. N. Koutsopoulos, "When do drivers yield to cyclists at unsignalized roundabouts? Empirical evidence and behavioral analysis," *Transportation Research Record Journal of the Transportation Research Board*, vol. 2520, pp. 25–31, 2015.

[12] Society of Automotive Engineers, *Operational Definitions of Driving Performance Measures and Statistics (Recommended Practice J2944)*, Society of Automotive Engineers, Warrendale, PA, USA, 2015.

[13] G. Markkula, J. Engström, J. Lodin, J. Bärgman, and T. Victor, "A farewell to brake reaction times? Kinematics-dependent brake response in naturalistic rear-end emergencies," *Accident Analysis & Prevention*, vol. 95, pp. 209–226, 2016.

[14] X. Wang, M. Zhu, M. Chen, and P. Tremont, "Drivers rear end collision avoidance behaviors under different levels of situational urgency," *Transportation Research Part C*, vol. 71, pp. 419–433, 2016.

[15] G. Markkula, V. T. Corp, O. Benderius, K. Wolff, and M. Wahde, "A review of near-collision driver behavior models," *Hunman Factors*, vol. 54, pp. 1117–1143, 2012.

[16] M. Green, "How long does it take to stop?" methodological analysis of driver perception-brake times," *Transportation Human Factors*, vol. 2, pp. 195–216, 2000.

[17] H. Summala, "Brake reaction times and driver behavior analysis," *Transportation Human Factors*, vol. 2, pp. 217–226, 2000.

[18] C. Llorca, A. Angel-domenech, F. Agustin-gomez, and A. Garcia, "Motor vehicles overtaking cyclists on two-lane rural roads: Analysis on speed and lateral clearance," *Safety Science*, vol. 92, pp. 302–310, 2017.

[19] Y. Matsui, S. Oikawa, and M. Hitosugi, "Analysis of car-to-bicycle approach patterns for developing active safety devices," *Traffic Injury Prevention*, vol. 17, pp. 434–439, 2016.

[20] M. Chen, X. Zhu, Z. Ma, and L. Li, "Driver brake parameters analysis under risk scenarios with pedalcyclist," SAE Technical Paper 2016-01-1451, 2016.

[21] G. Li, W. Wang, S. E. Li, B. Cheng, and P. Green, "Effectiveness of flashing brake and hazard systems in avoiding rear-end crashes," *Advances in Mechanical Engineering*, pp. 10–1155, 2014.

[22] J. Duan, R. Li, L. Hou et al., "Driver braking behavior analysis to improve autonomous emergency braking systems in typical Chinese vehicle-bicycle conflicts," *Accident Analysis & Prevention*, vol. 108, pp. 74–82, 2017.

[23] O. O. den Camp, A. Ranjbar, J. Uittenbogaard, E. Rosen, and S. Buijssen, "Overview of main accident scenarios in car-to-cyclist accidents for use in AEB-system test protocol," in *Proceedings of the International Cycling Safety Conference*, 2014.

[24] R. Fredriksson, K. Fredriksson, and J. Strandroth, "Pre-crash motion and conditions of bicyclist- to-car crashes in Sweden," in *Proceedings of the International Cycling Safety Conference 2014*, 2016.

[25] M. M. Minderhoud and P. H. L. Bovy, "Extended time-to-collision measures for road traffic safety assessment," *Accident Analysis & Prevention*, vol. 33, no. 1, pp. 89–97, 2001.

[26] S. Lefèvre, D. Vasquez, and C. Laugier, "A survey on motion prediction and risk assessment for intelligent vehicles," *ROBOMECH Journal*, vol. 1, pp. 1–14, 2014.